Segregation in multicomponent ceramic colloids during drying of droplets

Jian Wang and Julian R. G. Evans*
Department of Materials, Queen Mary, University of London, Mile End Road, London, E1 4NS, United Kingdom
(Received 11 August 2005; published 1 February 2006)

Studies of drying of colloidal droplets focus on unary particle systems. We report here the drying of binary and ternary powder suspensions. When multicomponent ceramic suspensions are deposited in the form of small drops (5 μl), particle segregation can occur on drying so that the upper surface of the powder residue does not match that of the bulk composition. We show that the segregation effect and the shape of the droplet residues are both related to the participation of particles in two types of flow during drying; radial flow toward the rim where the three-phase boundary becomes locked by a pile up of particles and secondly, recirculation flows in the remaining liquid driven by Marangoni stresses. Methods to control both shape and segregation are described. The phenomenon described is general and independent of the method of preparing the drops but the motivation is to obtain uniform drop shape and composition in thick film ceramic libraries in combinatorial ink-jet printing.

DOI: 10.1103/PhysRevE.73.021501 PACS number(s): 64.75.+g, 47.55.Kf, 83.80.Hj

I. INTRODUCTION

There are three stages of drying for a pure water droplet placed on a smooth polymer surface [1]. The contact diameter first remains constant while drop height and contact angle decrease. Then both the drop height and diameter decrease, maintaining a small contact angle. Finally, height, diameter and contact angle all decrease as the droplet volume diminishes to zero.

When the liquid contains fine particles this sequence is not followed. The three-phase boundary of a droplet of suspension is pinned by the rapid deposition of particles at the boundary on all but smooth, very low energy surfaces [2]. As a consequence, the radius remains constant and the drop shape loses sphericity or the cap recedes to the center leaving a "foot" as shown by Parisse and Allain [3]. Nonuniformities may develop in the spatial distribution of precipitated salts [4] and, as shown here, colloidal particles.

Maenosono *et al.* [5] describe a colloidal system in which a ring-shape multilayer formed at the drop periphery, with the ring width depending on the particle volume fraction. This lateral transport of carrier liquid has been observed directly by magnetic resonance microscopy during the drying of emulsion paints [6]. The process has been modeled by Routh and Russel [7] for a front of closely packed particles building up at the drying edge.

There is general agreement that radial flow occurs and is caused by the higher ratio of surface area to underlying liquid at the droplet edge. Even if the evaporating drop is placed on a pedestal surrounded by a liquid bath, the "foot" still develops [2]. Thus, lateral flow takes place in a sessile drop with a fixed periphery due to the geometrical requirements for volume depletion even if the mass transport coefficient is constant across the liquid-vapor boundary.

Haw *et al.* [8] observing unary powder systems, find that as the pile up at the edge grows, vertical circulation flows develop in the undried central region of the droplet followed by convectionlike cells in the horizontal plane. The packing of particles in the "foot" does not become fully dense until the liquid-rich cap has dried. The radial flow of liquid continues to supply the foot with liquid lost by evaporation. Only when the cap disappears and no replacement is available does the foot become well packed. Very recently, the circulation flows have been analyzed by Hu and Larson [9] in terms of the Marangoni stresses that result from surface tension gradients in an evaporating droplet.

Control of the geometry and compositional distribution of droplet residues is required in thick-film combinatorial libraries. These can be made by ink-jet printing methods that both mix multicomponent inks and dispense individual drops of discrete composition [10,11]. Likewise uniformity is needed in functional gradient materials produced by printing methods [12] and in any droplet based direct write method employing multicomponent suspensions.

II. EXPERIMENTAL DETAILS

The α-Al_2O_3 was Alcoa (Germany) A16-SG with average particle diameter 0.5 μm and density 3987 kgm^{-3}. Anatase TiO_2 (A-HR Tioxide Europe SA, France) was 99.0% purity with average particle diameter 0.15 μm and density 3850 kgm^{-3}. ZrO_2 (Pi-kem, Shropshire, UK) was free from stabilizing oxides (99.5%) with particle diameter 0.9 μm and density 5750 kgm^{-3}. This ternary was chosen because the x-ray $K\alpha$ energies are easily distinguished by energy dispersive x-ray spectrometry (EDS). The dispersant, Dispex A40 (Allied Colloids, Bradford, UK) is a solution of an ammonium salt of an acrylic polymer in water widely used to stabilize oxides in aqueous media.

A drop-on-demand printer (ProSys 4510, Cartesian Ltd, Huntingdon, Cambridge) quantitatively aspirates and dispenses ceramic suspensions to create different compositions. The process sequence for preparing ceramic compositions is illustrated in Fig. 1. The detail process has been described in Ref. [11]. Four compositions in the Al_2O_3-TiO_2-ZrO_2 system

*Email address: j.r.g.evans@qmul.ac.uk

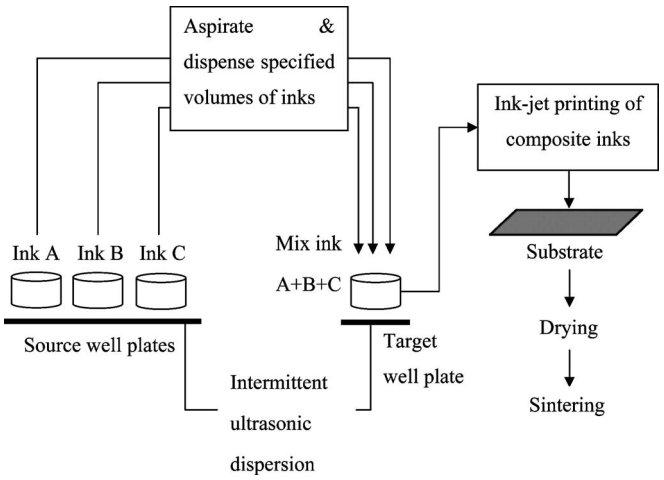

FIG. 1. The process of creating a ceramic mixture using the ink-jet printer.

(Table I rows 4 to 7) were made by mixing from three single component inks (Table I rows 1 to 3) and ink-jet deposition of aliquots of 5 μL on silicone release paper. After air drying for 3.6 ks, they were removed for EDS analysis without firing.

Drops in the ternary system were first deposited by ink-jet printing, but in order to show that the segregation is a general physical phenomenon and is independent of the printing process, all experiments were repeated by manual placement of the drops using dip wires. Manually deposited ceramic mixtures of the same nominal composition were mixed and subjected to ultrasonic disruption by an ultrasonic probe pulsed at 0.5 Hz and 50% amplitude for 1 ks to disperse clusters. This avoids contamination by milling media. Drops were placed on silicone release paper using a fine wire and treated thereafter as for the printed drops so that nominally identical printer-built and manually prepared compositions could be directly compared.

Both types of residue had a radius of 1–1.3 mm. The top surfaces, the lower surfaces and the cross sections were analyzed after coating with carbon as illustrated in Fig. 2. The microscope (SEM; Model 6300, JEOL, Tokyo, Japan) was equipped with an EDS system (Model eXL II, Oxford Instruments, Bucks, UK). Measurements were taken over an area approximately 150 μm$\times$150 μm for the surfaces and 50 μm$\times$50 μm for the cross section for a period of 100 s. These large dimensions avoid the spurious effects of agglomerates. The conditions were 20 kV acceleration voltage and 15 mm working distance. The data were corrected using INCA software (Oxford Instruments). Cobalt was used as a standard for calibration of the analyzer.

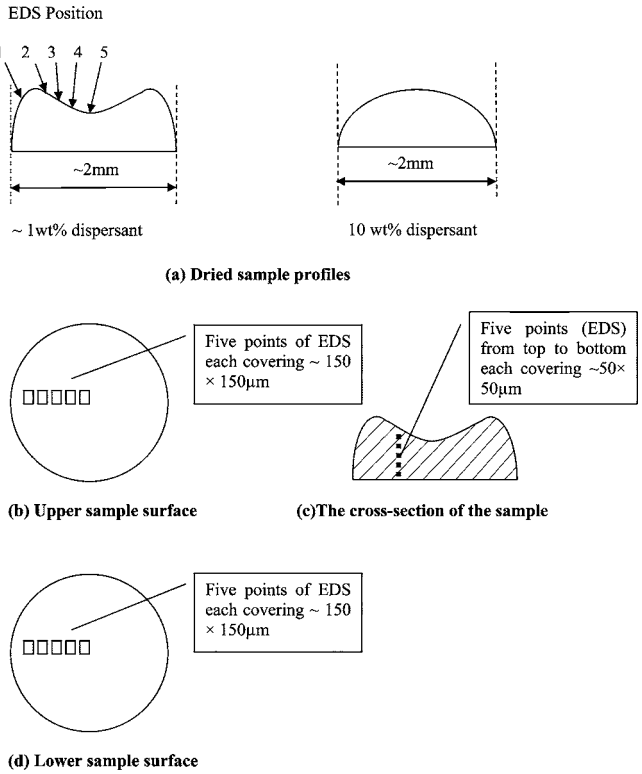

FIG. 2. Schematic plan for EDS analyses of droplet residues.

The viscosities were measured at 25 °C using a reverse flow U-Tube viscometer following BS 188:1977. The particle size distributions of powders were measured by Sedigraph (5100, Micromeritics Instrument corporation, Norcross, USA). Three 10 g Al_2O_3, ZrO_2, and TiO_2 single component ceramic suspension (Table I rows 1 to 3) were

TABLE I. The composition of ceramic suspensions.

Ink No.	Planned composition (wt. %)	Al_2O_3 powder (wt. %)	TiO_2 powder (wt. %)	ZrO_2 powder (wt. %)	DispexA40 (wt. %)	Distilled water (wt. %)
A	ZrO_2 100			38.83	1.52	59.65
B	TiO_2 100		29.93			70.07
C	Al_2O_3 100	30.46			0.77	68.77
D	Al_2O_3 50-ZrO_2 50	17.07		17.07	1.1	64.76
E	Al_2O_3 50-TiO_2 50	15.1	15.1		0.38	69.42
F	TiO_2 50-ZrO_2 50		16.9	16.9	0.66	65.54
G	Al_2O_3 25-TiO_2 25-ZrO_2 50	8.49	8.49	16.98	0.88	65.16
H	Al_2O_3 50-ZrO_2 50	17.07		17.07	10	55.86
I	TiO_2 50-ZrO_2 50		16.9	16.9	10	56.2
J	Al_2O_3 25-TiO_2 25-ZrO_2 50	8.49	8.49	16.98	10	56.04

TABLE II. Analysis by EDS of printer (P) and manually prepared (M) ceramic mixtures deposited on silicone release paper

Ink ID	Planned Composition (wt. %)	EDS analysis (wt. %)[a] Top surface P	Top surface M	Lower surface P	Lower surface M	Cross section P	Cross section M
D	ZrO_2 50	83±5	73±9	51±2	52±1	52±3	52±2
	Al_2O_3 50	17±5	27±9	49±2	48±1	48±3	48±2
E	Al_2O_3 50	84±13	81±16	53±3	50±3	51±3	49±3
	TiO_2 50	16±13	19±16	47±3	50±3	49±3	51±3
F	TiO_2 50	16±19	10±21	47±2	48±1	52±6	47±1
	ZrO_2 50	84±19	90±21	53±2	52±1	48±6	53±1
G	Al_2O_3 25	26±14	12±11	26±1	26±1	28±3	25±2
	TiO_2 25	6±7	9±12	24±2	24±0	24±2	24±2
	ZrO_2 50	67±21	79±22	50±2	50±1	48±3	51±3

[a]Average for five arrays at different positions shown in Fig. 2 with 95% confidence limit.

mixed and subjected to ultrasonic disruption by an ultrasonic probe at 0.5 Hz and 50% amplitude for 1 ks. Each suspension was diluted using 50 mL distilled water to reduce the concentration of powder to fit the requirements of the Sedigraph.

III. RESULTS

The EDS analyses of samples (Table II) show that whether the drops were mixed and printed automatically by the combinatorial printer or mixed by manual weighing and deposited using a fine wire, the EDS results for the lower surfaces and cross sections agreed with the planned compositions. For unpolished surfaces the agreement is within the error associated with the analysis method [13]. The top surfaces, on the other hand, were significantly different. Segregation of powders occurred in the upper surface region during drying.

The residues of these droplets formed 'doughnut' shapes and sometimes there was a through-thickness hole [Fig. 3(a)]. Although cracking of the residue sometimes occurred, EDS was only carried out on whole intact samples. The EDS results summarized in Table II are averaged from a positional array of assays systematically conducted along radial paths on the upper and lower surfaces and along the depth profile in cross sections (Fig. 2).

In each mixture, the EDS results at position 1 of the top surface (edge part) were consistently in better agreement with the planned composition than the results at positions 2, 3, and 4, a result which will become relevant when the segregation is interpreted. Tables III and IV (rows 1) give only two examples of the positional array but this effect was general. The analysis of large area scans of the cross section does not disclose how deep the surface nonuniformity is. Therefore, Fig. 4 provides a micrograph of the cross section of a residue prepared from ink F (TiO_2-ZrO_2 system) with

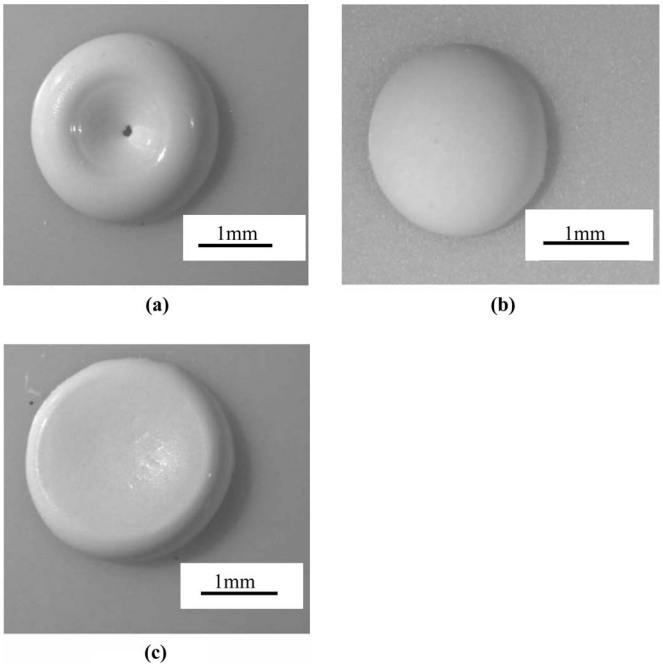

FIG. 3. The shape of droplet residues of ceramic inks: (a) doughnut shape (ink G); (b) dome shape (ink J), and (c) flat doughnut shape (ink F without dipsersant).

elemental mapping from regions at the drop centre to the edge. It shows ZrO_2 enrichment to a maximum depth of about 20 μm and the segregation layer became less thick towards the edge (see Table III, row 1).

Compositional nonuniformity and the "doughnut" shape with a possible hole at the center present serious problems both for thick film combinatorial studies of ceramics and for forming functionally graded products using direct ceramic ink jet printing. Interventions to solve these problems were launched and the interpretation of their results provides an explanation for the effects.

Deposition on porous substrates. In previous work [14], there was no segregation when droplets were deposited on dried, preplaced, porous layers of ink. Droplets were therefore manually placed on plaster of Paris which is used in slip casting and provides rapid separation of powder from its suspending fluid. Table V shows that all regions of these manually prepared ink mixtures deposited on this porous substrate agreed with the planned composition, although slightly larger errors were encountered for the analysis of the upper surface.

Similar enhancement of compositional uniformity by capillarity was obtained by placing drops on microporous cellulose nitrate membranes. Figure 5 compares the pore structure of plaster of Paris [Fig. 5(a)] with that of cellulose membrane [Fig. 5(b)]. Drops of inks F and G (Table I) were mixed and deposited manually onto cellulose nitrate membrane and samples were also printed thereon. These results confirm that fast drying by capillary flow into the substrate improves compositional homogeneity (Table VI); segregation is associated with slow drying by evaporation.

Effects of particle size and density. The simplest explanation for segregation is the selective sedimentation of either larger or more dense particles according to Stoke's law which gives the terminal velocity V_0 as

TABLE III. EDS analysis for droplet residues of ink composition F with different dispersant conditions, placed on silicone release paper.

Ink designation	Planned composition (wt. %)	EDS analysis (wt. %)														
		Top surface (edge→center)					Lower surface (edge→center)					Cross section (top→bottom)				
		1	2	3	4	5	1′	2′	3′	4′	5′	A	B	C	D	E
F with dispersant	TiO_2 50	36	1	1	3	9	47	48	49	49	48	46	47	48	48	47
	ZrO_2 50	64	99	99	97	91	53	52	51	51	52	54	53	52	52	53
F without dispersant	TiO_2 50	67	66	53	53	50	33	28	38	39	28	47	52	20	11	17
	ZrO_2 50	33	34	47	47	50	67	72	62	61	72	53	48	80	89	83
Dispersant on TiO_2	TiO_2 50	65	60	56	54	57	29	13	24	19	26	67	43	24	17	18
	ZrO_2 50	35	40	44	46	43	71	87	76	81	74	33	57	76	83	82
Dispersant on ZrO_2	TiO_2 50	35	5	5	5	5	27	28	32	29	27	20	48	81	84	20
	ZrO_2 50	65	95	95	95	95	73	72	68	71	73	80	52	19	16	80

$$V_0 = \frac{gd^2(\rho - \rho')}{18\eta}, \tag{1}$$

where d is the particle diameter, ρ is particle density, ρ' is the fluid density, and η is fluid viscosity. However, considering the average particle size and density of powders, it is clear that there is no evidence of preferred sedimentation; indeed there are examples where larger and denser particles ascend to the upper surface.

Using the particle size distributions shown in Table VII, 47% ZrO_2 powder but only 2.7% TiO_2 is greater than 0.7 μm. ZrO_2 also has much higher density (5750 kg m^{-3}) than TiO_2 (3850 kg m^{-3}). For the 50% ZrO_2–50% TiO_2 ink, ZrO_2 should be depleted on the upper surface due to preferential sedimentation but as shown by EDS (Table III, row 1), TiO_2 almost disappeared on the upper surface of the residue. This segregation cannot be explained by preferential sedimentation. The same conclusion can be drawn from the other three compositions in Table II. There is no indication of coarser or denser particles settling out.

Effect of dispersant. In order to assess the effects of dispersant, compositions D and F (described in Table I) were prepared without dispersant (which was replaced by the same amount of distilled water). These suspensions were manually prepared and mixed for 1 ks with the ultrasonic probe and deposited on silicone release paper.

The results for composition F (TiO_2-ZrO_2 system) with and without dispersant are compared in Table III rows 1 and 2. The difference in these composition scans is striking. Without dispersant, the upper surface, instead of showing excess zirconia, now presents a slight deficit. No effect of radial distribution can be detected. This implies that the segregation of ZrO_2 to the upper surface seen before, was associated with the presence of dispersant. In contrast, the lower surface is now rich in ZrO_2: an effect that can indeed be attributed to preferential sedimentation. Such sedimentation is clearly seen in the cross section which has a steady increase in ZrO_2 from top to bottom.

The results for ink D (ZrO_2-Al_2O_3 system) with and without dispersant are compared in Table IV rows 1 and 2. In the case of the ink with dispersant, ZrO_2 is richer on the upper

TABLE IV. EDS analysis for droplet residues of ink compositions D placed on silicone release paper.

Ink designation	Planned composition (wt. %)	EDS analysis (wt. %)														
		Top surface (edge→center)					Lower surface (edge→center)					Cross section (top→bottom)				
		1	2	3	4	5	1′	2′	3′	4′	5′	A	B	C	D	E
D with dispersant	ZrO_2 50	69	75	75	82	65	51	53	52	52	51	52	52	55	51	51
	Al_2O_3 50	31	25	25	18	35	49	47	48	48	49	48	48	45	49	49
D without dispersant	ZrO_2 50	52	51	51	50	51	51	50	51	51	51	52	52	53	52	51
	Al_2O_3 50	48	49	49	50	49	49	50	49	49	49	48	48	47	48	49
Dispersant on Al_2O_3	ZrO_2 50	33	18	25	25	26	59	62	62	58	50	23	17	34	82	80
	Al_2O_3 50	67	82	75	75	74	41	38	38	42	50	77	83	66	18	20
Dispersant on ZrO_2	ZrO_2 50	42	51	52	52	53	38	47	45	43	42	41	38	37	42	56
	Al_2O_3 50	58	49	48	48	47	62	53	55	57	58	59	62	63	58	44

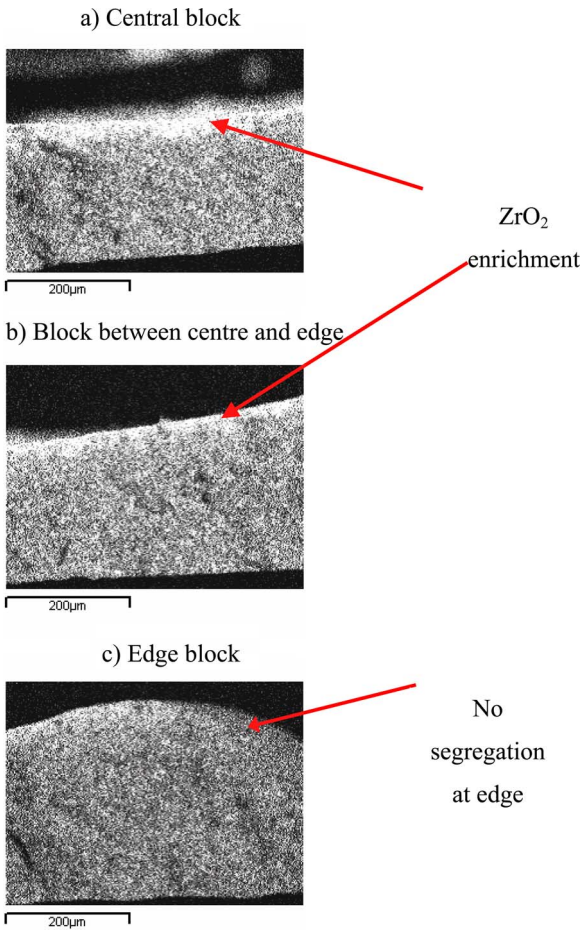

FIG. 4. (Color online) Elemental mapping showing the depth of the segregated ZrO_2 layer on the upper surface of residue from ink F. (a), (b), and (c) are taken from positions identified on Fig. 2(a) as 5, 3, and 1, respectively.

surface. Without dispersant, there is no segregation; the upper surfaces, cross sections, and lower surfaces of residues agree well with the planned composition. In this case, there is no preferential sedimentation. This result is further confirmation that segregation on the upper surface is associated with the presence of dispersant.

Removal of excess dispersant. When dispersant is added to a suspension it tends to adsorb strongly on the solid surface until saturation is reached and the excess remains in solution. The excess can be removed by centrifuging the suspension, removing the supernatant, and redispersing the powder in the same mass of liquid. The amount of dispersant in solution can be found by drying and weighing.

TABLE V. Average EDS results for ink mixtures deposited on plaster of Paris.

Ink ID	Planned Composition (wt. %)	EDS analysis (wt. %)[a]		
		Top surface	Lower surface	Cross section
G	Al_2O_3 25	22±5	23±1	23±2
	TiO_2 25	25±5	26±0	28±2
	ZrO_2 50	53±10	50±1	49±2

[a]Average for five arrays at different positions shown in Fig. 2 with 95% confidence limits.

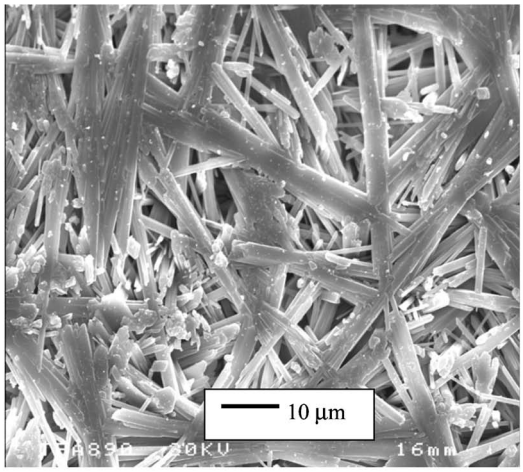

(a) SEM picture of calcium sulphate (Plaster of Paris) substrate

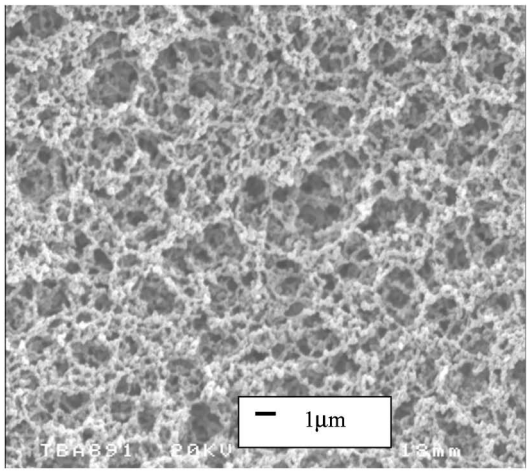

(b) SEM picture of cellulose nitrate membranes

FIG. 5. Porous substrates used for rapid separation of powder from suspending fluid; (a) plaster of Paris and (b) cellulose nitrate membrane.

TABLE VI. Average EDS results for manually prepared (M) and machine mixed and printed (P) ink mixtures deposited on microporous cellulose nitrate membrane.

Ink ID	Planned composition (wt. %)	EDS analysis (wt. %)[a]					
		Top surface		Lower surface		Cross section	
		P	M	P	M	P	M
F	TiO_2 50	50	48	53	51	49	47
	ZrO_2 50	50	52	47	49	51	53
G	Al_2O_3 25	25	23	27	26	26	25
	TiO_2 25	24	24	26	26	25	22
	ZrO_2 50	51	53	47	48	49	54

[a]Average for three arrays at different positions.

TABLE VII. Particle size distributions for the three powders.

Low diameter (μm)	Cumulative mass coarser (%)		
	ZrO_2	Al_2O_3	TiO_2
3	1.2	3.7	0.0
0.7	47.0	20.6	2.7
0.4	63.8	45.0	23.9
0.3	70.1	60.4	46.5
0.2	76.9	77.7	73.3
0.1	85.5	91.2	92.4

Using ink F, TiO_2 powder was first mixed with half the amount of water and the full amount of dispersant. The resulting TiO_2 ink contained 1.31 wt. % Dispex. After centrifuging for 30 min, gravimetric analysis showed that half the dispersant remained in the supernatant which was replaced with the same mass of distilled water into which TiO_2 was redispersed. ZrO_2 powder, mixed with the other half of water without dispersant was then added. This produces a mixed ink with 50 wt. % TiO_2–50 wt. % ZrO_2 in which the dispersant is initially adsorbed on the TiO_2. EDS analysis of residues (Table III, row 3) show ZrO_2 depletion on the upper surface and evidence of preferential sedimentation of ZrO_2 in the cross section and on the lower surface.

The ZrO_2 powder in ink F was then treated with dispersant instead. The results (Table III, row 4) show TiO_2 depletion on the upper surface. However, preferential sedimentation of ZrO_2 was also found in the lower surface. This combined effect is due to the wider particle size range of the ZrO_2 powder; larger particles are still able to sediment.

This selective procedure was then followed with ink D (50 wt. % Al_2O_3–50 wt. % ZrO_2). Dispersant was first added only to the Al_2O_3 and the excess removed before adding ZrO_2 free from dispersant. The results (Table IV row 3) indicate ZrO_2 depletion on the upper surface and evidence of preferential sedimentation of ZrO_2 on the lower surface and in the cross section.

Then the dispersant was added to ZrO_2 powder first, excess was removed and Al_2O_3 ink without dispersant added. The results (Table IV, row 4) show that for this mixture, the upper surface is close to the as-planned composition with only slight excess of ZrO_2, but there are signs of Al_2O_3 sedimentation on the lower surface not picked up in the large area scans for the cross section.

Removing excess dispersant does not provide a general solution to the segregation problem but it illustrates the sensitivity of segregation to preferential adsorption on specific powders; an effect that can over-ride preferential sedimentation under Stoke's law. The important observation was that the powder to which dispersant was preferentially attached was always richer on the upper surface of dried droplets and this general observation helps to explain the phenomenon of separation (*vide infra*).

Use of excess dispersant. The inks used in these experiments contain around 1 wt. % dispersant; sufficient to achieve stability during the period of printing. In the next step, inks H, I, and J (Table I) were prepared with large amounts of dispersant (10 wt. %). These were manually prepared, mixed for 1 ks with the ultrasonic probe and deposited on silicone release paper. EDS analysis of these residues, described in Table VIII, show neither sedimentation nor segregation, the whole body of the residues has uniform composition as planned.

TABLE VIII. EDS analysis of droplet residues of multicomponent ceramic colloids containing excess dispersant showing uniform composition.

Ink No.	Dispex (wt. %)	Planned Composition (wt. %)	EDS analysis (wt. %)[a]		
			Top surface	Lower surface	Cross section
H	10	Al_2O_3 50	50±3	52±1	51±2
		ZrO_2 50	50±3	48±1	49±2
I	10	TiO_2 50	50±4	46±1	47±2
		ZrO_2 50	50±4	54±1	53±2
J	10	Al_2O_3 25	25±1	26±0	24±1
		TiO_2 25	25±1	23±0	24±1
		ZrO_2 50	50±1	51±0	52±1

[a]Average for five arrays at different positions shown in Fig. 2 with 95% confidence limits.

These inks presented another difference. The residues of ink H, I, J retained a dome shape [Fig. 3(b)] without the lateral movement of powder to the periphery. No cracking was found in such residues. The large amount of dispersant increased the kinematic viscosity of these inks (from 1.5 to 3.7 $mm^2\ s^{-1}$ for inks D and H and from 1.4 to 11.4 $mm^2\ s^{-1}$ for inks F and I). Adding a larger amount of dispersant provides a generally sound solution to the segregation problem based on formulation rather than substrate selection, achieving a uniform residue of the planned composition. Furthermore, the shape of residue was a simple guide to compositional uniformity.

IV. DISCUSSION

The final compositional distribution in residues is set up during drying. For a particle in a droplet of ceramic suspension, there are at least four types of particle motion: (i) sedimentation due to gravity, (ii) Brownian motion due to collisions with fluid molecules, (iii) lateral migration of particles to form a "foot" at the periphery of the drop, and (iv) fast recirculation flows that occur in the remaining liquid part of the drop. In unary suspensions, these have been observed by Haw *et al.* [8], modeled by Hu [9] and can easily be seen in the optical microscope using oblique illumination and have the appearance of vigorous stirring with an element of chaos. These movements can be restricted by surrounding particles, by dispersant, and by flocculation behavior. On the basis of (iii) and (iv), we interpret both the shape and the segregation effects described here.

From the particle size distributions in Table VII, the particle size increases for the series TiO_2, Al_2O_3, and ZrO_2.

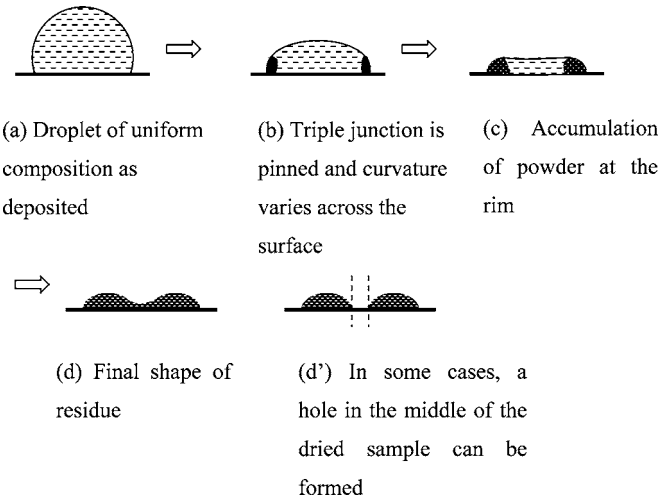

FIG. 6. Schematic representation of the observed drying process for droplets from suspensions containing ~1 wt. % dispersant.

Table II indicates that in the Al_2O_3-TiO_2, ZrO_2-TiO_2, Al_2O_3-ZrO_2, and TiO_2- Al_2O_3-ZrO_2 systems, powder with the larger particle size is concentrated on the upper surface. Preferential sedimentation fails to explain the segregations seen on the upper surfaces in these experiments.

In a well-dispersed suspension, particles participate in the radial flow, piling up at the periphery and forming a foot which grows as drying proceeds and leaving a hollow central region which may even produce a hole. A similar situation prevails in the spray drying of ceramic slurries; discrete droplets from well-dispersed slurries in which particles retain mobility during drying, form irregular shaped agglomerates with a central hole. Suspensions with a tendency to flocculate, form dense spherical agglomerates [15]. In the present work, the use of large amounts of dispersant increases viscosity and is likely to impede particle mobility by chain entanglement effects. Sessile drops from these inks dry to leave dome shapes [Fig. 3(b)] with uniform planned composition.

For droplets from suspensions containing ~1 wt. % dispersant (inks D, E, F, and G), particles have high mobility in the suspension. Visual observation of reflectivity, transparency and the appearance of a discontinuity in the surface [Fig. 3(c)], suggest that a higher packing density of powder builds up at the three phase boundary as generally observed [2–6]. The suspension on the rim continues drying as liquid migrates from interior regions to the periphery under capillary forces, eventually forming a "doughnut" shape in which the centre is depleted and sometimes leaving a hole. The process is illustrated as Fig. 6.

This does not explain the segregation effect, which can only be understood by looking also at the liquid region of the sessile drop contained within the surrounding foot. As described by Haw *et al.* [8], this region contains vigorous recirculation flows. These can be seen in the optical microscope with oblique illumination. These flows are attributed to Marangoni stresses resulting from surface tension gradients and thermal gradients associated with evaporation of liquid and have been modeled [9]. As the drop dries, this region shrinks while the more densely packed "foot" grows.

A particle in suspension can either join the "foot" or participate in the recirculation flows in the central pool. We argue that the better dispersed particles participate in the flow while the weakly dispersed particles join the "foot" and in this way segregation develops on the upper surface where the well-dispersed particles accumulate. The process is shown schematically in Fig. 7.

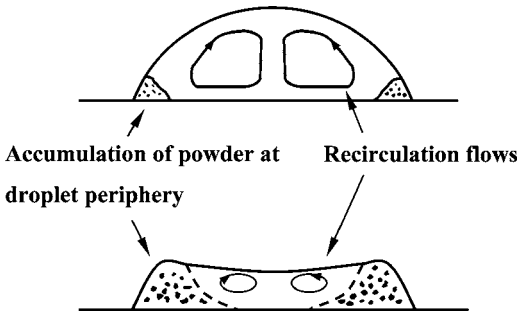

FIG. 7. Schematic diagram of radial and recirculation flows that are responsible for particle segregation.

This explanation is consistent with the geometry of residues, with Fig. 4 and with the observation that at assay position 1 (Tables III and IV row 1), the composition is closer to that planned than at positions 2–4. Position 1 became isolated from the liquid pool at an earlier stage. The explanation is consistent with the observations that the better dispersed particles always appeared in excess at the top irrespective of their density or particle size. Position 5 is not necessarily worse than position 1 as seen in Table 4 row 1. When a hole is formed, position 5 is a very thin section from which the final liquid, containing well-dispersed particles, is drawn laterally by capillary action into position 4 as drying comes to an end.

The behavior of inks containing no dispersant depended on the particular powders in combination. For the ZrO_2-TiO_2 system, the TiO_2 was a fine powder while ZrO_2 was a comparatively coarse powder as deduced from SEM images and particle size distributions (Table VII). When there was no dispersant, ZrO_2 powder began to sediment, most TiO_2 was still dispersed in the water. These droplets dried to leave a much flatter "doughnut" shape as shown in Fig. 3(c). After drying, TiO_2 was richer on the upper surface while ZrO_2 powder was preferentially sedimented on the lower surface as evidenced by EDS results (Table III, row 2).

For the Al_2O_3-ZrO_2 system, after the ultrasonic probe was switched off, the powders began to flocculate. The suspension appeared to become more viscous forming a paste rather than a liquid. This is typical of flocculated suspensions [16]. These drops ended as a dome with uniform planned distribution of powder (Table IV rows 2) and it seems reasonable to speculate that this is because a three-dimensional flocculated network prevents particles from participating the two modes of liquid flow. Using flocculation as a means to prevent segregation would provide a solution but it is incompatible with the need to produce low viscosity suspensions stable against sedimentation for ink-jet printing.

It is instructive to compare the ZrO_2-TiO_2 system under three conditions: dispersant added to both powders, no dispersant added, and dispersant attached only to ZrO_2. When dispersant is attached to both ZrO_2 and TiO_2 powders and excess is left in solution, residues of droplets are "doughnut"

shaped with ZrO_2 powder richer on the upper surface and the lower surface agreeing with the planned composition (Table III, row 1). Without dispersant, the residues of droplets are flatter doughnut shapes with preferential sedimentation of ZrO_2 powder (Table III, row 2). With dispersant attached only to ZrO_2, residues of droplets have both types of segregation; ZrO_2 powder is richer on the upper surface yet preferential sedimentation of larger ZrO_2 particles (Table III row 4) shows up on the lower surface.

In the Al_2O_3-ZrO_2 system, when dispersant is only attached to ZrO_2 with no excess available for Al_2O_3 in the solution, residues of droplets are "doughnut" shaped with much more uniform composition (Table IV, row 4). The ZrO_2 is slightly denser and coarser than the Al_2O_3 so the effects of sedimentation and ascent in the liquid zone tend to cancel.

V. CONCLUSIONS

Residues of droplets from mixed multicomponent ceramic suspensions which were well-dispersed were found to present "doughnut" shapes with segregation on the upper surface on drying. By depositing on porous substrates, segregation was prevented. The same effect can be obtained on impermeable substrates by using excess dispersant which increases viscosity and may induce entanglement flocculation. Residues of such droplets retained the dome shape providing a better geometry for combinatorial measurement methods and had uniform and planned composition.

The segregation effect is not due to preferential sedimentation unless dispersant addition is restricted. Segregation is due to the partitioning of particles between the growing peripheral "foot" that develops during drying and the diminishing liquid pool which contains vigorous recirculation flows. Better dispersed particles remain in the pool and hence are found in excess on the upper surface of residues. Less well dispersed particles join the "foot" earlier in the drying process.

Using excess dispersant significantly increased the viscosity and reduced the mobility of particles and hence segregation. The same effect was seen in flocculating suspensions without dispersant. By centrifuging a discrete suspension, removing the supernatant and redispersing the powder in the same mass of liquid, it is possible to obtain mixtures in which only one type of powder is treated with dispersant. In such drops, the better dispersed powder segregates to the upper surface. Thus the final residue shape and the presence of segregation are connected and are attributed to particle mobility in two flow regimes; radial flow to the drop periphery and recirculation flows in the central pool.

ACKNOWLEDGMENTS

The authors are grateful to the Engineering and Physical Science for funding this work under Grant No. GR/R06977.

[1] M. E. R. Shanahan and C. Bourges, Int. J. Adhes. Adhes. **14**, 201 (1994).
[2] R. D. Deegan, O. Bakajin, T. F. Dupont, G. Huber, S. R. Nagel, and T. A. Witten, Phys. Rev. E **62**, 756 (2000).
[3] F. Parisse and C. Allain, Langmuir **13**, 3598 (1997).
[4] J. J. Guo and J. A. Lewis, J. Am. Ceram. Soc. **82**, 2345 (1999).
[5] S. Maenosono, C. D. Dushkin, S. Saita, and Y. Yamaguchi, Langmuir **15**, 957 (1999).
[6] R. D. Deegan, O. Bakajin, T. F. Dupont, G. Huber, S. R. Nagel, and T. A. Witten, Nature (London) **389**, 827 (1997).
[7] A. F. Routh and W. B. Russel, AIChE J. **44**, 2088 (1998).
[8] M. D. Haw, M. Gillie, and W. C. K. Poon, Langmuir **18**, 1626 (2002).
[9] H. Hu and R. G. Larson, Langmuir **21**, 3972 (2005).
[10] J. R. G. Evans, M. J. Edirisinghe, P. V. Coveney, and J. Eames, J. Eur. Ceram. Soc. **21**, 2291 (2001).
[11] J. Wang and J. R. G. Evans, J. Mater. Res. **20**, 2733 (2005).
[12] J. Wang and J. R. G. Evans, J. Comb. Chem. **7**, 665 (2005).
[13] V. D. Scott, G. Love, and S. J. B. Reed, *Quantitative Electron-Probe Microanalysis* (Ellis Horwood, London, 1995), p. 93.
[14] M. M. Mohebi and J. R. G. Evans, J. Am. Ceram. Soc. **86**, 1654 (2003).
[15] G. E. Fair and F. F. Lange, J. Am. Ceram. Soc. **87**, 4 (2004).
[16] P. C. Hidber, T. J. Graule, and L. J. Gaukler, J. Am. Ceram. Soc. **79**, 1857 (1996).